

Investigating the between-event variability of the site response from KiKnet data in Japan

Conference Paper**Author(s):**

[Perron, Vincent](#) ; Bergamo, Paolo; Fäh, Donat

Publication date:

2021

Permanent link:

<https://doi.org/10.3929/ethz-b-000505143>

Rights / license:

[In Copyright - Non-Commercial Use Permitted](#)

INVESTIGATING THE BETWEEN-EVENT VARIABILITY OF THE SITE RESPONSE FROM KIKNET DATA IN JAPAN

Vincent Perron¹, Paolo Bergamo¹, and Donat Fäh¹

¹ Swiss Seismological Service, ETH Zürich, Switzerland (vincent.perron@sed.ethz.ch)

ABSTRACT

Uncertainties in seismic hazard analysis are very large and critical for the hazard at long return period. An important part of this uncertainty is, however, epistemic and could be reduced by improving our understanding and subsequently the models. Site effect is a major component of seismic hazard analysis, which significantly participate to the overall uncertainty. In this study, we try to understand what is controlling the between-event uncertainty of the site response.

We estimate the amplification function from Standard Spectral Ratio (SSR) at three SSMNet stations in Switzerland and the surface-to-borehole spectral ratio at 60 KiKnet stations having recorded several hundreds of earthquakes. The preliminary step is the automatic quality control, phase picking, Fourier spectrum computations and signal-to-noise ratio verification of more than two million traces. Artificial outliers are identified and discarded before performing the statistical analysis. First of all, our results confirm that amplification factors at any site or frequency are well approximated by a log-normal distribution. Based on that it is possible to use the confidence interval to determine the variation of the mean computed from subset of events.

Using the confidence interval, we propose an analytic equation to estimate the number of events to be recorded to have a certain stability in the mean amplification function estimation. We found that at least 20 earthquakes should be used to limit the variation of the mean amplification function below 30% for every station and frequency. We finally estimate that the ground motion intensity (PGA) has no influence on the anelastic site amplification functions as far as the site behave linearly.

Keywords: seismic hazard analysis, site effects, site response variability, statistical distribution

INTRODUCTION

Site effects can significantly increase the seismic hazard and risk locally. Unconsolidated deposit such as thick and soft sediments in sedimentary basins are prone to strongly amplify the ground motion. Site effects are caused, among others, by the impedance reduction during the propagation to the earth surface, the 1D, 2D and 3D resonances, and the edge-generated surface waves. In turn, the site response can vary significantly from one earthquake to another. At large ground motion levels, non-linear effects in specific soils will increase the aleatory uncertainty as well.

The between-event variability of the site response is very small when estimated from 1D SH site-response analysis because it is a strong simplification of the real phenomena. Contrarily, approaches based on direct observations from real earthquake recordings are appropriated for analyzing the variability of the site response. One of the most commonly used approaches to measure the site response is the standard spectral ratio (SSR) introduced by Borchardt (1970). It consists in performing the ratio in the Fourier domain between the signal recorded at one station on sediments with the signal obtained at another station located nearby on a stiffer site condition (i.e., a rock site) for the same earthquake.

The SSR is computed for each component individually or for the mean of the two horizontal component and can be noted as:

$$SSR_i(f) = \frac{FAS_{Si}(f)}{FAS_{Ri}(f)}, \quad 1$$

where $SSR_i(f)$ is the SSR for the i th component as a function of the frequency f , FAS_{Si} and FAS_{Ri} are respectively the Fourier amplitude spectra at the site and at the reference computed over the i th component.

The ground motion amplification at the reference station is assumed to be negligible, that is to say, equal to one at every frequency. In practice it is never the case, so the site's response is not absolute but is always relative to the considered reference. The SSR approach is based on the assumption that the earthquake source and wave propagation are the same between the site and the reference and thus cancelled out when performing the spectral ratio between the two. This assumption is valid if the site-to-reference distance (R_{STA}) is much smaller than the hypocentral distance (R_h). In practice adopting $R_h > 10R_{STA}$ is considered to be enough, even though a certain part of the SSR variability can probably be explained by a remaining influence of the source and of the propagation.

One of the main limitations of the SSR is of having a rock outcropping susceptible to be used for the reference site located not too far from the considered site of interest. An alternative to the classical SSR is to deploy one station at the earth surface on sediments and the second at the same location but in a borehole deep enough to reach the geophysical bedrock. This so-called surface-to-borehole spectral ratio (SBSR) approach has the advantage of solving the between-station distance limitation but introduces some new difficulties due to the seismic waves reflection at the earth surface. The upgoing and downgoing waves are indeed fully constructive at the earth surface while it can be destructive at certain frequencies at depth. However, in the context of analyzing only the variability of the site response, the downgoing waves interaction can reasonably be neglected.

The main goal of this work is to improve our knowledge related to the observed aleatory variability of ground-motion amplification. We estimate the SSR and SBRS amplification function for stations of the Swiss strong motion network (SSMNet) and of the Japanese KiKnet network having recorded hundreds of earthquakes. We use this large amount of data to determine the statistical distribution of the site amplification. Based statistical distribution definition, we propose an analytic equation predicting the variation of the mean amplification according to the standard deviation and to the number of events. We also estimate the dependence on the mean amplification functions of the ground motion intensity, measured as the Peak Ground Acceleration (PGA).

METHOD AND RESOURCES

In Switzerland, we develop a waveform database covering the time period 1998-jan to 2019-sep. Waveforms at each Swiss site were selected according to a magnitude-distance filter. In Japan, the database is covering the time period 1997-oct to 2016-mar. We follow the same procedure for every computation of the site response in Switzerland and Japan. This procedure is the following:

1. Automatic quality checks of earthquake recordings and automatic picking of the P and S wave arrival (T_P , T_S) through a time-frequency analysis;
2. Selection of earthquake with hypocentral distance at least 5 times the inter-station distance;
3. Selection of the signal window between T_P and $3.3T_S - 2.3T_P$, and of the noise window before T_P and of same duration as the signal window. Site and reference use the same time windows;
4. Computation of the Fourier Amplitude Spectra (FAS) for the noise and for the signal window;
5. Computation of the horizontal mean FAS using the quadratic mean: $\sqrt{\frac{N^2 + E^2}{2}}$
6. Smoothing and resampling of the horizontal mean FAS on a logarithmic scale using the Konno and Ohmachi (1998) approach with b-value of 50;
7. Estimation of the Signal-to-Noise Ratio (SNR);
8. Selection of earthquakes with $SNR > 5$ over at least a 10 Hz frequency band both at the site and at the reference;

9. Spectral ratio computation between the horizontal mean FAS at the site and at the reference for each earthquake;
10. Estimation of the between-events geometric mean and standard deviation at each frequency;
11. Detection of outliers as group of samples of probability <math><0.1\%</math> over a frequency band larger than 1 octave;
12. Outliers are discarded and the geometric mean and standard deviation are recomputed;

Figure 1 shows an example of the surface-to-borehole spectral ratio computation in Japan. The map shows the location of the site (green triangle) and the epicenters of the selected earthquakes (yellow-to-red dot). The top right panels present the FAS for the noise (black lines) and for the earthquake recording at the reference (green lines) and at the site (blue lines). The bottom-left panel indicates the SNR at the reference (green lines) and at the site (blue lines), as well as the number of earthquakes with $\text{SNR} > 5$ (red line) as a function of frequency. Bottom right panels show the distribution of the horizontal and vertical SBSR as a function of frequency. The color scale indicates the density of lines, each line corresponding to the SBSR of one single earthquake.

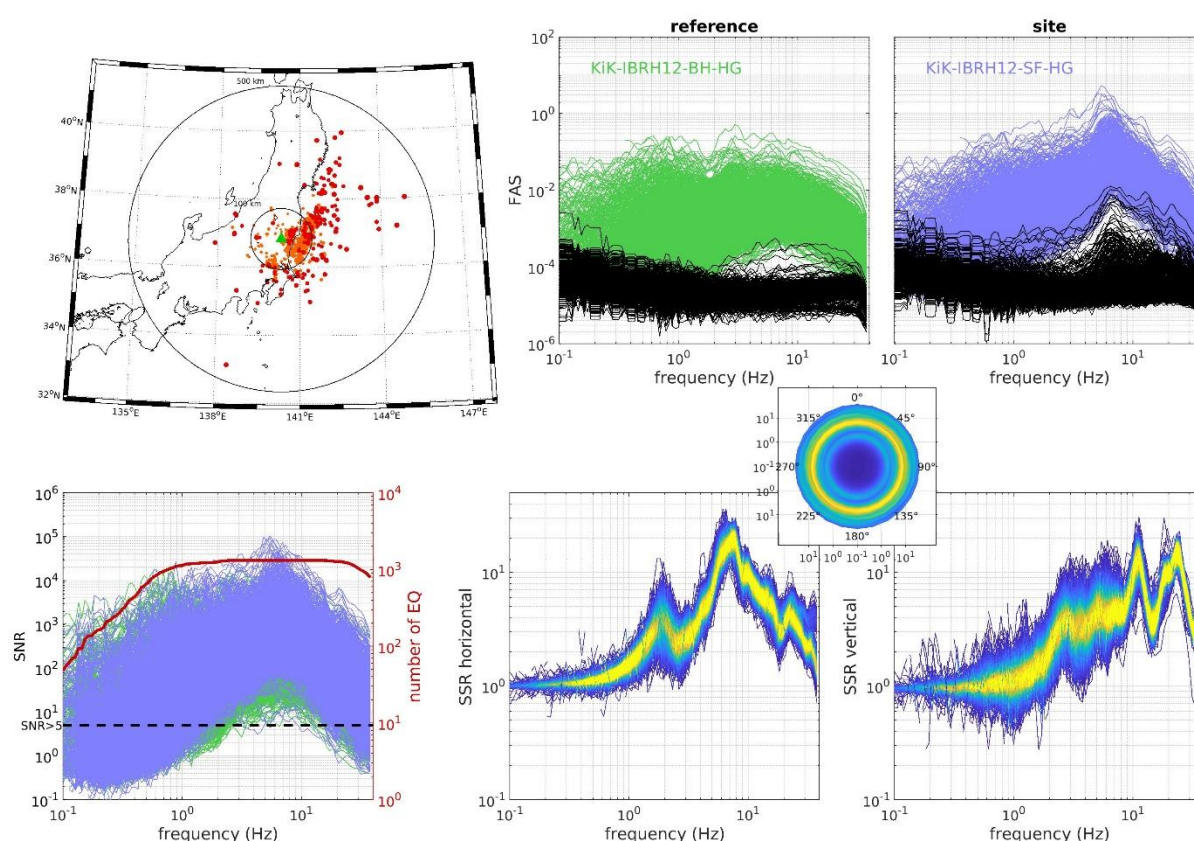


Figure 1. Example of the surface-to-borehole spectral ratio computation at KiKnet station IBRH12 in Japan.

SSR AND SBSR RESULTS

In total, SSR are estimated from 3 pairs of stations where approximately 100 good quality earthquakes have been recorded in Switzerland, and SBSR are computed from 60 pairs of surface-to-borehole stations with up to 2000 good quality earthquakes in Japan. Figure 2 and Figure 3, respectively show the distribution of the SBSR for 60 pairs of surface-to-borehole stations in Japan and the SSR for the 3 pairs of surface stations in Switzerland. Figure 4 provides a summary of the number of good quality earthquake, geometric mean, and geometric standard deviation as a function of frequency in Japan (grey curves) and in Switzerland (red curves).

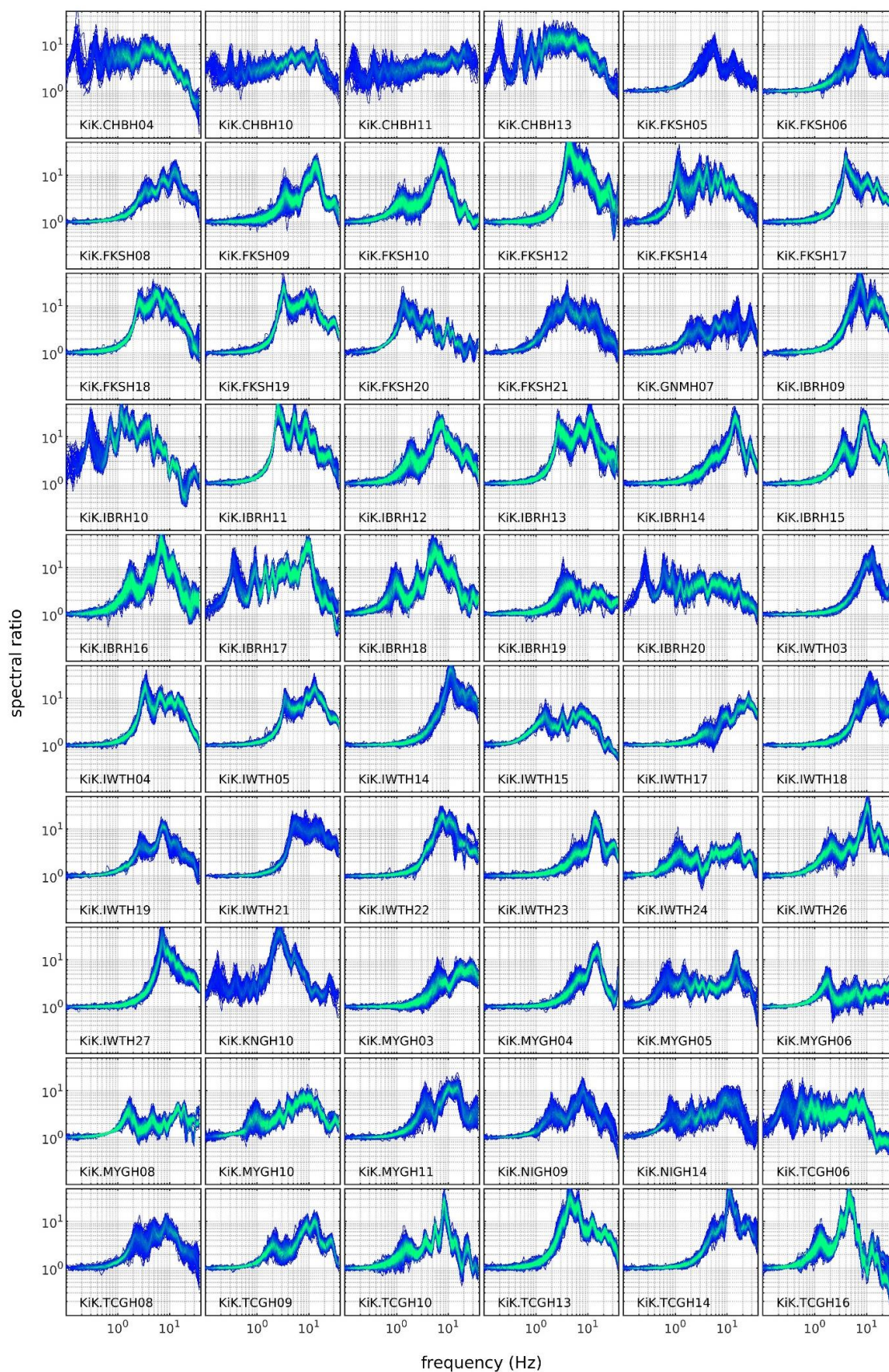


Figure 2. Amplification function computed from the surface-to-borehole spectral ratio between 60 pairs of stations in Japan. The color from dark blue to light green indicates an increasing density of curves, each curve corresponding to one single earthquake. Red circles indicate parts of the amplification function with unexpected distribution shape.

It is clear on Figure 2, Figure 3, and Figure 4 that the amplification functions are different from one site to another, both in terms of mean and standard deviation. It reflects the differences on the geological conditions of the sites, which determine, among other, the fundamental resonance frequency of the site (f_0), here corresponding to the first peak on the amplification function. The between-events standard deviation can also vary drastically from one site to another and depending on the frequency. In Japan, we can separate the amplification functions in two groups: a first group with $f_0 > 0.5$ Hz, with amplification function equal to one and low standard deviation (close to 1.05) for frequency below f_0 ; a second group with f_0 below the minimum frequency of the analysis here (0.1 Hz), and having significant amplification and high variability at low frequency. It is also clear that the variability of the site response is in average higher in Switzerland than in Japan. This is probably due, in Switzerland, to the relatively high site-to-reference distances and to non-negligible site effects of the surface reference station. In Japan we can observe some anomalies (no log-normal distribution) in the amplification function at high frequency (i.e., for stations: KiK-IBRH13; KiK-IBRH17; KiK-TCGH13). It is not possible to clearly determine its origin, but from our experiences this is very probably an artificial artefact due to coupling issues of the borehole instrumentation.

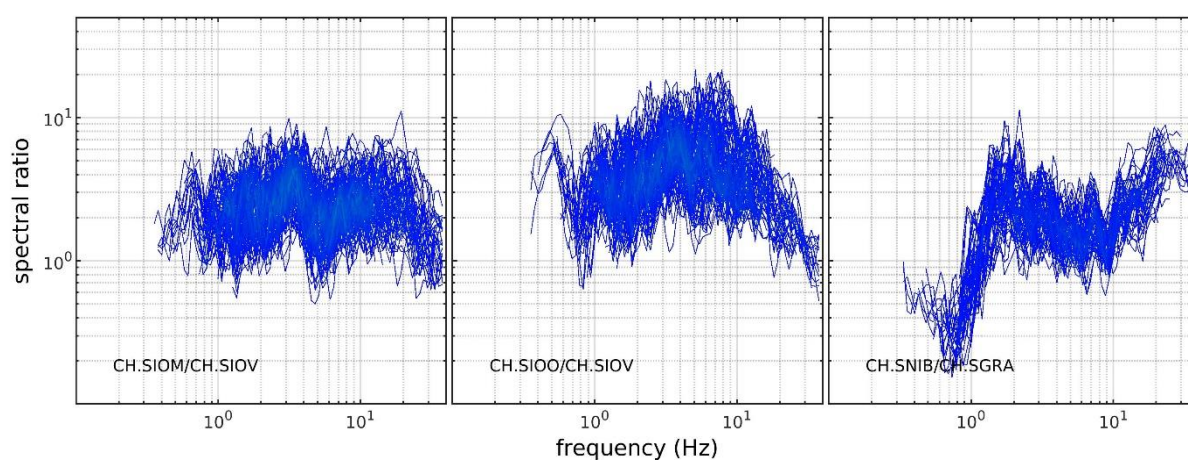


Figure 3. Amplification function computed from the standard spectral ratio between 3 pairs of stations in Switzerland. The color from dark blue to light blue indicates an increasing density of curves, each curve corresponding to one single earthquake.

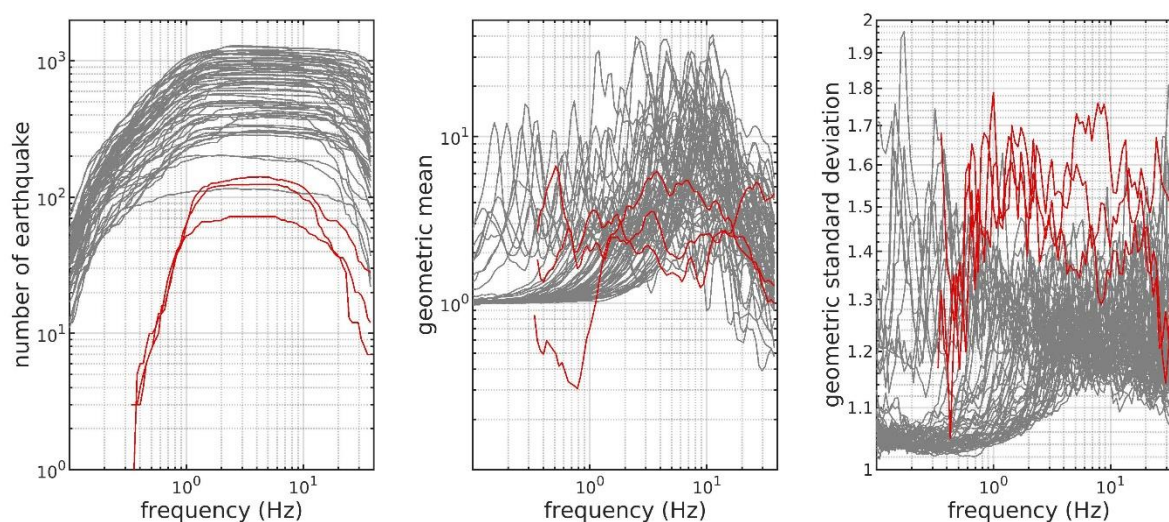


Figure 4. Number of good quality earthquake (left panel), between-events geometric mean (central panel), and between-events geometric standard deviation (right panel) as a function of frequency for 60 surface-to-borehole spectral ratio in Japan (grey curves) and 3 standard spectral ratio in Switzerland (red curves).

DISTRIBUTION OF THE BETWEEN-EVENTS SITE RESPONSE VARIABILITY

As we have seen in the previous section, both the mean amplification function and the between-events site response variability as a function of frequency are dependent of the geological characteristics of the site itself. However, the nature of the site response distribution is the same independently of the site or of the frequency and has been shown to be well modelled by a log-normal distribution. In other words, the distribution of the logarithm of the relative amplification of the ground motion between two sites is Gaussian.

To qualitatively verify the log-normal distribution of the site response at every frequency, the quantile-quantile plot (Q-Q plot) and the histogram are represented at frequencies 0.5, 1.0, 2.5, 5.1, 9.9 and 20.6 Hz on Figure 5. The shape of the histograms of the logarithm of the amplification factors represents a Gaussian and Q-Q curves of every site at every frequency are well aligned along the 1/1 line, in particular in the interval $\pm 2\sigma$ to the mean. These indicate that the site response is very well approximated by log-normal distribution at least up to $\pm 2\sigma$. Beyond 2σ , the few non-natural outliers and the limited number of samples increase the scatter of the Q-Q curves, meaning that the log-normal distribution is still valid but interpretations made out of it are less reliable.

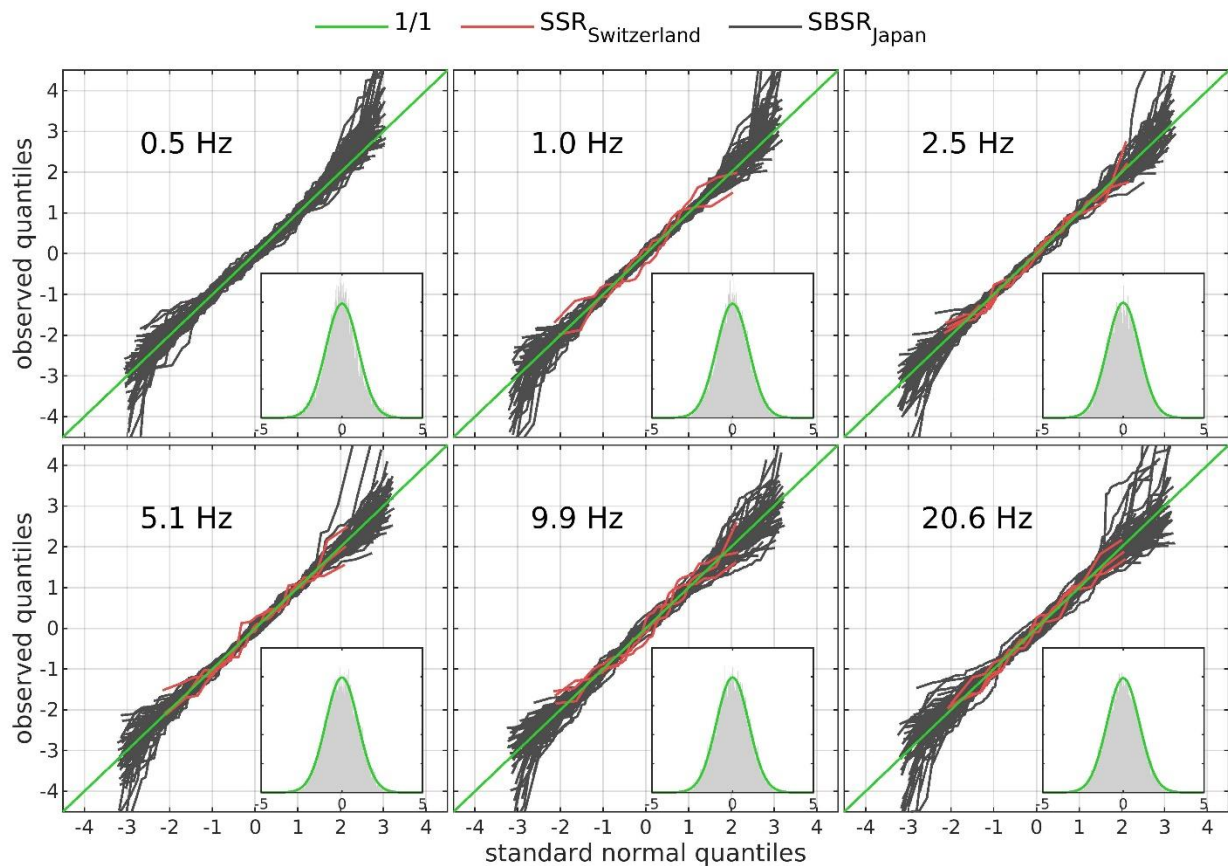


Figure 5. Quantile-quantile plot of the logarithm of the amplification factors for 60 surface-to-borehole spectral ratio in Japan (grey curves) and 3 standard spectral ratio in Switzerland (red curves) at 6 different frequencies (one panel per frequency). On each panel, the histogram (grey area) of the standard normal distribution computed from the logarithm of the amplification factors at all site at the corresponding frequency is compared to the best normal distribution fit (green curve).

Proving the log-normal distribution of the amplification function is important because then peculiar statistical properties apply. For example, if a variable x is normally distributed then the distribution of sample means (\bar{x}_n) computed from subset of n samples also are normally distributed. One major output of that is the confidence interval (I_c). Given that a sample mean (\bar{x}_n) and unbiased standard deviation (s_n) have been estimated from a finite number of samples (n), the confidence interval is the interval

inside which the population mean (μ) for an infinite number of samples has a certain confidence level to be included in. It is defined as

$$Ic_{1-\alpha\%} = \left[\bar{x}_n - Z_{\alpha/2} \frac{S_n}{\sqrt{n}} ; \bar{x}_n + Z_{\alpha/2} \frac{S_n}{\sqrt{n}} \right], \quad 2$$

$Z_{\alpha/2}$ is the critical value which defines the confidence level ($1 - \alpha$). For a normal distribution and a confidence level of 95%, $Z_{0.025}$ is equal to 1.96. However, because the number samples can be sometime very limited (i.e., only a few earthquakes have been recorded), it is preferable to use the Student distribution, also called t-distribution. This distribution correctly accounts for small number of samples and tend to a normal distribution as the number of samples increases. For a student distribution, the formulation of $Ic_{1-\alpha\%}$ is the same (equation 2), but the estimation of $Z_{\alpha/2}$ is different, as it now also depends on n . The evolution of $Z_{\alpha/2,n}$ as a function of n and for the confidence level 68%, 95%, 99% and 99.9% is given on Figure 6, left panel.

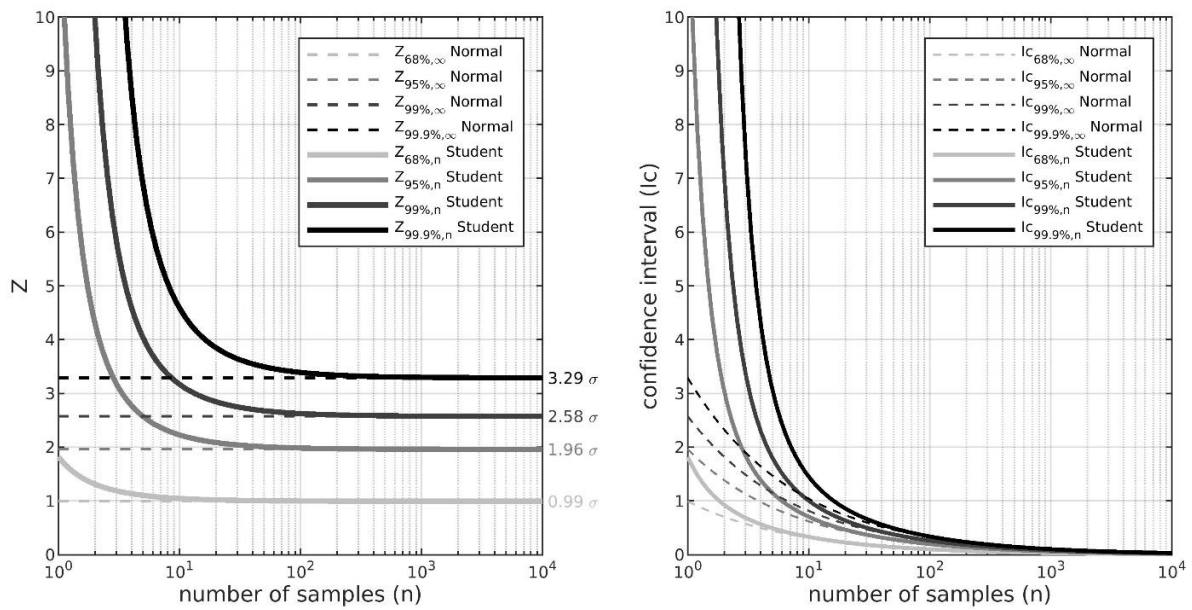


Figure 6. Critical value Z (left panel) and confidence interval (right panel) as a function of the number of samples for the confidence level 68%, 95%, 99% and 99.9% for the standard normal distribution (dashed lines), and the standard Student distribution (solid lines).

In the following, we will keep using the notation \bar{x}_n and s_n for the measured sample geometric mean and standard deviation, while μ and σ represent the population geometric mean and standard deviation of the distribution. For an infinite number of samples the two notations becomes equivalent: $\bar{x}_\infty = \mu$ and $s_\infty = \sigma$. Moreover, we will only focus on the confidence level of 95%, because the 95% confidence interval corresponds approximately to the interval comprised between $[-1.96\sigma, 1.96\sigma]$, which in turn corresponds to portion where the Q-Q plot best fit the 1/1 line (Figure 5). As the distribution is not normal but log-normal, we accordingly modified the confidence interval formulation. The 95% confidence interval for a log-Student distribution is finally:

$$Ic_{95\%} = \left[\bar{x}_n * \frac{1}{\exp\left(Z_{0.025,n} \frac{\ln(s_n)}{\sqrt{n}}\right)} ; \bar{x}_n * \exp\left(Z_{0.025,n} \frac{\ln(s_n)}{\sqrt{n}}\right) \right], \quad 3$$

With \bar{x}_n and s_n respectively the sample geometric mean and standard deviation computed as

$$\bar{x}_n = \exp\left(\frac{1}{n} \sum_{i=1}^n \ln(x_i)\right), \quad 4$$

$$s_n = \exp \left(\sqrt{\frac{1}{(n-1)} \sum_{i=1}^n (\ln(x_i) - \ln(\bar{x}_n))^2} \right), \quad 5$$

Figure 6 (right panel) shows the evolution of $Ic_{68\%}$, $Ic_{95\%}$, $Ic_{99\%}$ and $Ic_{99.9\%}$ for a standard normal and standard Student distribution ($\mu = 0$; $\sigma = 1$). It illustrates the very rapid reduction of the confidence interval as the number of samples increases, from more than 10σ when $n < 10$ to less than 1σ when $n > 10$.

VARIABILITY OF THE MEAN AMPLIFICATION FUNCTION AS A FUNCTION OF THE NUMBER OF EVENTS

Some questions which arise when evaluating the amplification function at a specific site are: Is the number of earthquakes recording sufficient to accurately estimate the amplification function? Which minimal number of earthquake (n_{min}) should be used to evaluate the site response?

Based on the confidence interval definition (equation 3), it is clear that the variability of \bar{x}_n depends both on s_n and n . Because s_n is site and frequency dependent (Figure 4), n_{min} is by consequence also site and frequency dependent. In other words, there is no unique value of n_{min} which can be considered for every site response analysis in the world. Oppositely, the property of the site response to be log-normally distributed is universal. It is then possible to determine n_{min} for any site response analysis, based on the log-normal distribution assumption and on the use of the confidence interval definition.

Provided that the geometric mean \bar{x}_n and standard deviation s_n of the site response has been measured at a particular site over a certain number of earthquakes n , it is possible to determine in which confidence interval the population mean for an infinite number of events μ has a certain confidence level (here 95%) to be included in. It is also possible to predict what will be the reduction of this interval if the number of earthquake increase. In the same way, it is possible to determine the number of earthquakes required to limit to a certain level the width of the interval where μ has a 95% probability to be found within. The width of the interval is independent to the \bar{x}_n and can be defined from equation 3 by

$$C_{95\%} = \exp \left(Z_{0.025,n} \frac{\ln(s_n)}{\sqrt{n}} \right), \quad 6$$

$C_{95\%}$ is the coefficient of variation between μ and \bar{x}_n such as $\frac{\bar{x}_n}{C_{95\%}} \leq \mu \leq C_{95\%} \bar{x}_n$ with a 95% probability. It is now possible to estimate the minimum number of earthquakes required to limit the variation between μ and \bar{x}_n below a certain coefficient $C_{95\%}$ as

$$n_{min} = \left(Z_{0.025,n} \frac{\ln(s_n)}{\ln(C_{95\%})} \right)^2, \quad 7$$

For example, if the amplification at 1 Hz has been measured from $n = 10$ earthquakes with a geometric standard deviation of $s_{10} = 1.5$, we can estimate the minimum number of earthquake n_{min} to have $C_{95\%} = 1.2$ (20% of variation) with a probability of 95% as

$$n_{min} = \left(Z_{0.025,10} \frac{\ln(s_{10})}{\ln(C_{95\%})} \right)^2 = \left(2.26 \frac{\ln(1.50)}{\ln(1.20)} \right)^2 = 25.31 \rightarrow 26 \text{ earthquakes}$$

It is important to note that for a Student distribution, $Z_{0.025,n}$ is function of n . $Z_{0.025,n}$ will decrease very rapidly as the number of measured earthquakes increases (Figure 6). Using equation 7 and measured s_n (Figure 4), n_{min} is computed for every site in Switzerland and Japan, and at every frequency. The results are reported on Figure 7. As already discussed, n_{min} is dependent on s_n , so that it is variable for the different site and frequency. Swiss SSRs have the highest uncertainty and logically required the highest number of earthquakes for a given coefficient of variation $C_{95\%}$. Table 1 summarizes the minimum number of earthquakes which is valid for 99% of our sites at every frequency as a function of $C_{95\%}$.

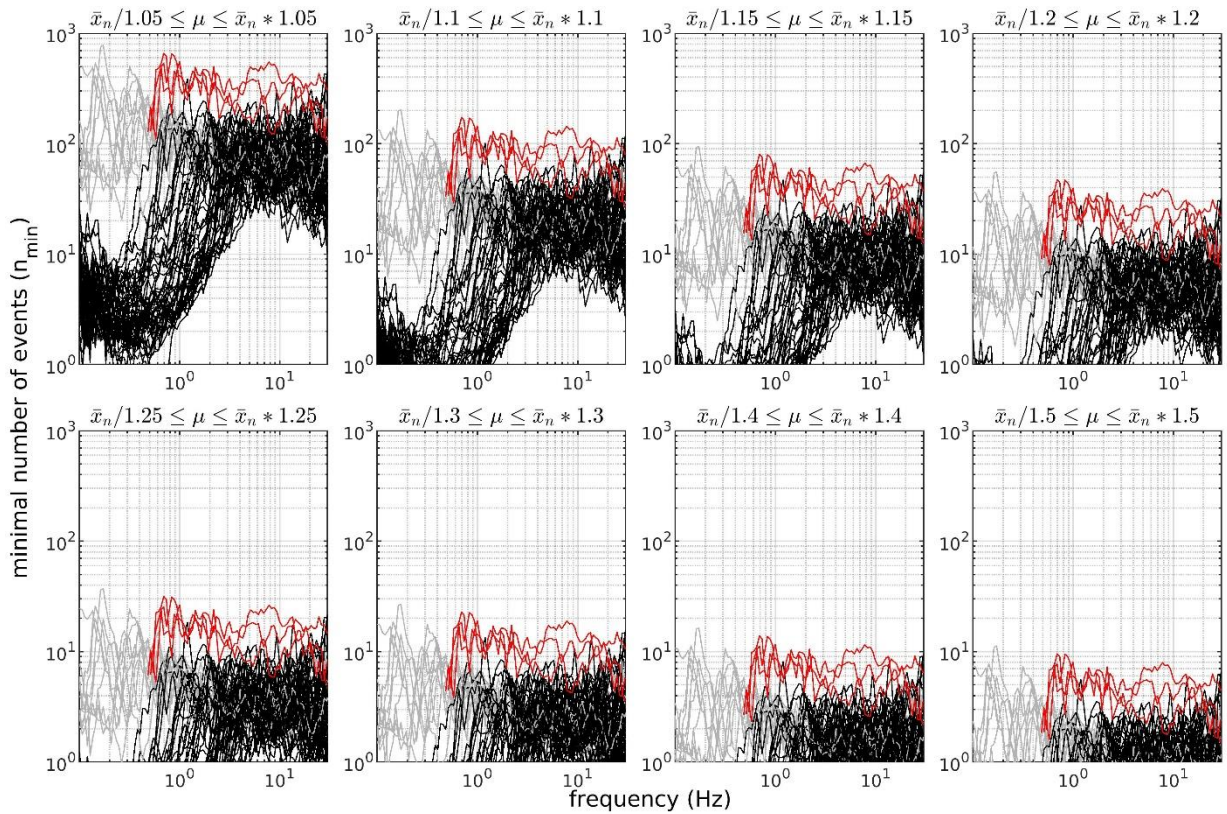


Figure 7 – Minimum number of earthquakes as a function of frequency for the coefficient of variation $C_{95\%}$ equal to 1.05, 1.10, 1.15, 1.20, 1.25, 1.30, 1.4, and 1.5 (panels). KiKnet stations with $f_0 > 0.5$ Hz are represented in black, KiKnet stations with $f_0 < 0.1$ Hz are represented in grey, and Swiss stations are represented in red.

Table 1. Minimum number of earthquakes n_{min} as a function of the coefficient of variation $C_{95\%}$

$C_{95\%}$	1.05 (5%)	1.10 (10%)	1.15 (15%)	1.20 (20%)	1.25 (25%)	1.30 (30%)	1.40 (40%)	1.50 (50%)
n_{min}	550	160	70	40	25	20	12	8

For 10 earthquakes recorded, the estimation of the mean is only 50% accurate approximately ($C_{95\%} = 1.5$). It is possible to reduce this uncertainty to 30% by recording 20 events ($C_{95\%} = 1.3$). Depending on the desired limit for the coefficient of variation of the mean, one can make own estimations of the minimum number of earthquakes by using equation 7.

It has to be highlighted that s_n is the key parameter for the estimation of n_{min} . If s_n is wrongly determined, so will be n_{min} . One difficulty to have a representative determination of s_n is how to deal with the outliers. Including erratic outliers will artificially increase s_n , while removing natural outliers from rare events will truncate the true distribution and reduce s_n . Another difficulty is that looking only at the value of n_{min} might not be enough for all sites. One could claim that because the site response has been measured from 30 earthquakes, the statistical significance of the result is good and the coefficient of variation of the mean is low. However, if all the events present the same characteristic and location because they belong to the same cluster of events, then the significance of the results is not good and the true variability of the site response might be strongly underestimated. For instance, Perron (2017), shows that around 50% of the between events site response variability in 2D and 3D basins comes from lighting effect which strongly depends on the source location. This implies that both the number of events and their spatial distribution around the site should be considered in site response analysis.

DEPENDENCE OF THE SITE RESPONSE VARIABILITY TO THE INTENSITY OF THE GROUND MOTION

The dependence of the site response to the intensity of the ground motion is a complex research topic which interests the community for several decades. The non-linear behavior of unconsolidated soil to strong ground motion solicitation is of major interest in engineering seismology. Non-linearity tends to reduce the fundamental resonance frequency of the site, leading to an increase of the hazard at low frequency and a decrease at high frequency. In extreme cases it can also lead to liquefaction phenomena. One question often arises when speaking about empirical site effects assessment which is: is the measured amplification function from weak ground motion representative for site response to strong ground motion? To address this question, we compute the equivalent of the standard normal distribution ($\mu = 0$, $\sigma = 1$) for every individual amplification function at all sites in Switzerland and Japan as

$$Z_i = \frac{\ln(x_i) - \ln(\bar{x}_n)}{\ln(s_n)}, \quad 8$$

This common standard normal distribution formulation allows to use the site response of every site together. $Z_i(f)$ represent the i^{th} normalized amplification function normally distributed with $\bar{x}_n = 0$, and $s_n = 1$. Together, it represents about 28 000 normalized amplification functions obtain from thousands of earthquakes recorded at 63 pairs of stations (3 Swiss sites and 60 Japanese sites). For each normalized amplification function, we computed on the corresponding waveforms the horizontal mean Peak Ground Acceleration (PGA).

Figure 8 shows the number of events per frequency, the distribution of the PGA and the normalized amplification function for four PGA bins ([0.001 0.01], [0.01 0.1], [0.1 1], and [1 10] m/s²). First it should be said that the number of events drastically varies from one PGA bins to another. This explains the apparent differences when looking at the normalized amplification function (black curves) of the different bin. We observe that the normalized amplification function for every PGA bin can be all explain by the standard normal distribution, which indicates that no non-linear behavior is observed here. The mean is fairly equal to 0 and the standard deviation equal to 1 for every frequency for every bin. This demonstrates that the linear site response is independent of the ground motion intensity. Therefore, if we consider a specific site having a linear behavior, the amplification function observed from a magnitude 1 earthquake will be the same as the one for a magnitude 6 earthquake, all other things been the same. This highlight the importance and the validity of using recording of low-to-moderate earthquakes to assess the anelastic amplification function for larger earthquakes.

CONCLUSIONS

Site effect is a major contributor to the seismic hazard, and its evaluation at specific sites of interest generally requires the recording of several earthquakes. We address here the question of the site response variability and of the minimum necessary number of earthquakes to be recorded.

To address this question, we carefully compute empirical amplification functions at 60 KiKnet sites from several hundred earthquakes and at 3 Swiss sites from several tens of earthquakes. We performed statistical analysis on the amplification function to estimate the geometric mean and standard deviation, and more importantly to determine the distribution law of the amplification factor at each frequency. Independently to the site and to the frequency, we find that the log-normal distribution is a very good approximation for the site response. Based on that we develop a strategy to estimate the minimum number of earthquakes from the confidence interval definition. We first demonstrate the validity of the use of the confidence interval to model the uncertainty on the geometric mean estimation. Based on the confidence interval, we provide the analytic formula to estimate the minimum number of earthquakes to be recorded, as a function of the between-events standard deviation (equation 7). We used it on the Swiss and Japanese amplification function and determine, among others, that with a 95% probability: the mean varies by less than 50% for 10 earthquakes, and less than 30% for 20 events. As a general rule, 10 uncorrelated earthquakes is the minimum number of earthquakes to be considered, but the higher the number of earthquakes the lower the uncertainty on the geometric mean site response assessment.

The linear site response is observed to be independent to the intensity of the ground motion. In other words, assessing the site response from recording of low PGA and low magnitude earthquakes, provides the same amplification functions as from recording of high PGA and large magnitude earthquakes, as far as the soil behaves linearly.

It is very important to point out that satisfying the minimal number of earthquakes by itself is not sufficient. The selected earthquakes should be uncorrelated and as much evenly distributed around the site as possible to cover the entire variability of the site response. One should not use only earthquakes belonging to a single cluster of events.

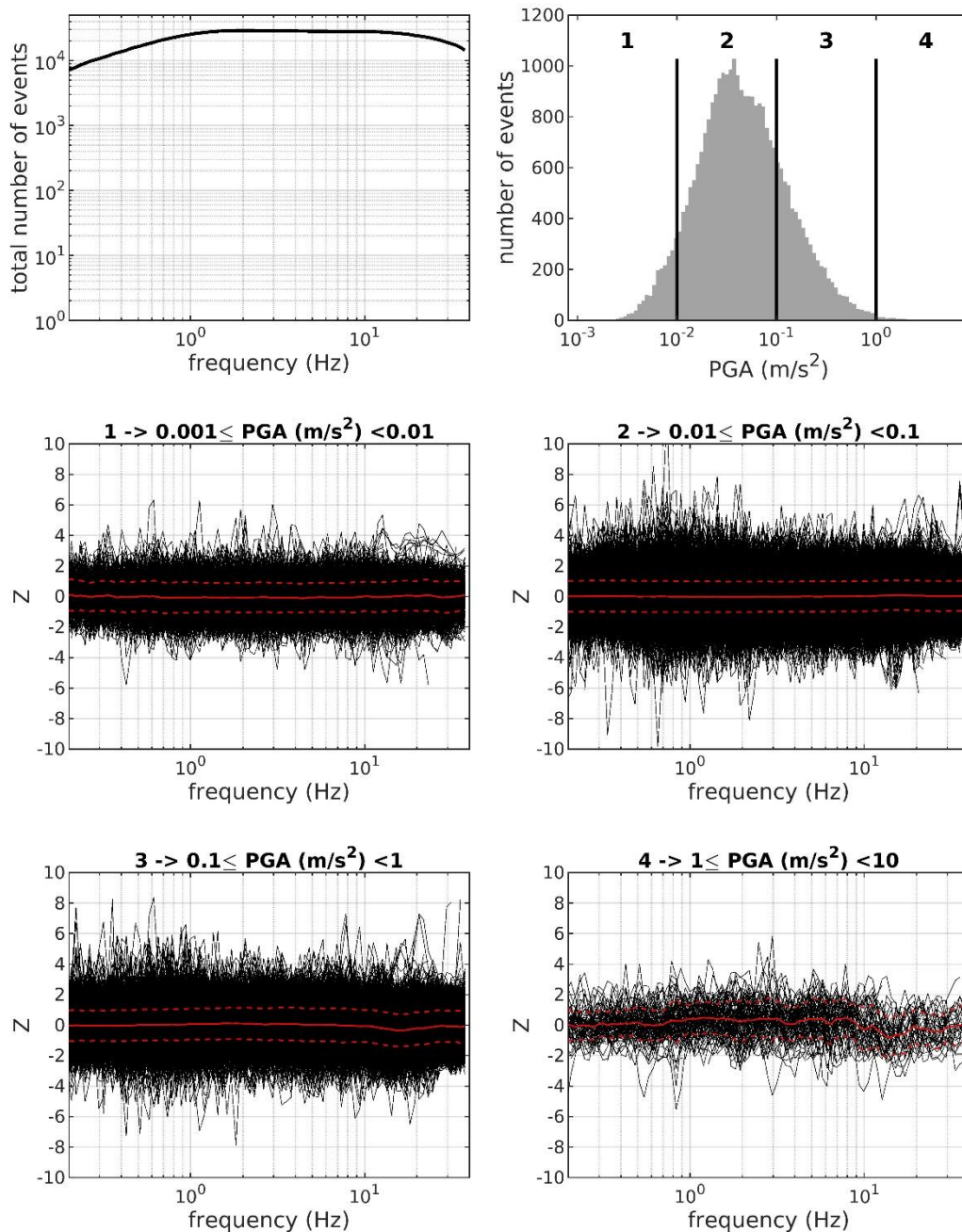


Figure 8 – Top left panel: Total number of normalized amplification function obtain from 3 Swiss SSR distribution and 60 SBSR Japanese distribution and as a function of frequency. Top right: Histogram of the Peak Ground Acceleration (PGA) distribution. From middle left to bottom right panel: normalized amplification function for four PGA bins and as a function of frequency. The mean and mean plus/minus standard deviation are represented with solid red line and dotted red lines respectively.

REFERENCES

- Borcherdt, R.D. (1970). "Effects of local geology on ground motion near San Francisco Bay". *Bull. Seismol. Soc. Am.* **60**, 29–61.
- Konno, K., Ohmachi, T. (1998). "Ground-motion characteristics estimated from spectral ratio between horizontal and vertical components of microtremor". *Bull. Seismol. Soc. Am.* **88**, 228–241.
- Perron, V. (2017). Apport des enregistrements de séismes et de bruit de fond pour l'évaluation site-spécifique de l'aléa sismique en zone de sismicité faible à modérée (PhD thesis). *Université Grenoble Alpes*, Grenoble, France.